



HAL
open science

Influence of Lanthanum Coatings on a Model 330 Alloy (Fe–35Ni–18Cr–2Si) Oxidation at High Temperatures

Henri Buscail, Christophe Issartel, Frédéric Riffard, Raphaël Rolland, Sébastien Perrier, Alexandre Fleurentin

► **To cite this version:**

Henri Buscail, Christophe Issartel, Frédéric Riffard, Raphaël Rolland, Sébastien Perrier, et al.. Influence of Lanthanum Coatings on a Model 330 Alloy (Fe–35Ni–18Cr–2Si) Oxidation at High Temperatures. *Oxidation of Metals*, 2014, 81 (1-2), pp.127-138. 10.1007/s11085-013-9423-x . hal-01628272

HAL Id: hal-01628272

<https://uca.hal.science/hal-01628272>

Submitted on 3 Nov 2017

HAL is a multi-disciplinary open access archive for the deposit and dissemination of scientific research documents, whether they are published or not. The documents may come from teaching and research institutions in France or abroad, or from public or private research centers.

L'archive ouverte pluridisciplinaire **HAL**, est destinée au dépôt et à la diffusion de documents scientifiques de niveau recherche, publiés ou non, émanant des établissements d'enseignement et de recherche français ou étrangers, des laboratoires publics ou privés.

Influence of Lanthanum Coatings on a Model 330 Alloy (Fe-35Ni-18Cr-2Si) Oxidation at High Temperature

Henri Buscail^a, Christophe Issartel^a, Frédéric Riffard^a, Raphaël Rolland^a, Sébastien Perrier^a, Alexandre Fleurentin^b

^a*Clermont Université – UdA - LVEEM, 8 rue J.B. Fabre, BP 70219, 43006 Le Puy en Velay, France*

^b*CETIM, 52 av Félix Louat, BP 80067, 60304 Senlis, France*

henri.buscail@udamail.fr, raph43@hotmail.fr, christophe.issartel@udamail.fr, frederic.riffard@udamail.fr ;
sebastien.perrier@udamail.fr ; alexandre.fleurentin@cetim.fr

Abstract. The influence of a lanthanum sol-gel coating on the chromia scale adherence has been studied on the 330 alloy (Fe-35Ni-18Cr-2Si) oxidized at 900°C, in air. Argon annealing of lanthanum sol-gel coatings have been performed at various temperatures. Kinetic results show that lanthanum sol-gel coatings lead to a lower oxidation rate compared to blank specimens. On blank 330 specimens scale spallation is observed after cooling to room temperature. On the non-annealed sol-gel coated specimen and the argon annealed specimens at 600, 800 or 1000°C, the oxide scale formed at 900 °C is adherent after 48 hours isothermal oxidation. The adherent oxide scales are convoluted. It results from an anionic and a cationic mixed diffusion process in the chromia scale. Thermal cycling tests on lanthanum the sol-gel coated specimen show that the oxide scale remains adherent after 250 cycles. It is concluded that argon annealing of the lanthanum sol gel coating is not necessary to improve the scale adherence.

Keywords: Lanthanum, Sol-gel coating, Chromia, Alloy 330 (Fe-35Ni-18Cr-2Si)

INTRODUCTION

Metal dusting is a catastrophic carburisation phenomenon that occurs at temperatures of 450–850°C in atmospheres of high carbon activity. Even though some high-silicon alloys resist to metal-dusting environments [1], carburization is the main reason of conveyor units degradation due to a quick alloy weakening. The resistance of alloys to corrosion, including metal dusting, relies on the formation of a dense, adherent oxide layer that separates the alloy from the corrosive environment. For such an oxide layer to be protective, it must achieve full surface coverage, be crack-free and be established before significant material degradation has occurred. An adherent oxide scale can act as a carbon diffusion barrier and improve the alloy carburization resistance [2-5]. Chromia Cr₂O₃ is considered as a protective oxide formed at high temperature. Stevens et al. have shown that a Fe-35Ni-18Cr-2Si alloy can be used as a resistance heating-element material and it has been studied in the 1000 and 1300°C temperature range [6]. Nevertheless, at temperatures higher than 1100°C the chromium oxide CrO₃ evaporation occurs. In this case, chromium depletion is observed in the oxide scale and in the alloy. The concentration of elements in the protective oxide was found to be both temperature and time dependent. Chromia is stable at low temperature (< 1100 °C) and was found to evaporate at higher temperatures and longer oxidation time, thereby increasing nickel and iron concentrations. On the basis of changes in the chemical composition of the oxide film, together with scaling, the failure of heating-element wire by the development of hot spots can be explained. At failure both long-term (low temperature < 1000°C) and shorter-term tests (temperature > 1000°C) were found to have oxidized to the same depth. This can be explained on the basis of a depletion of chromium, which occurred at the oxide-alloy interface, and becomes insufficient for a healing process. A previous study has shown that in the 800-1000°C temperature range, the niobium containing 330Cb alloy oxidation leads to a chromia scale acting as a good diffusion barrier under isothermal conditions [7]. The external manganese chromite subscale has no influence on the diffusion properties of the main chromia scale. It is expected that the manganese chromite can limit the

1
2
3
4 chromia scale evaporation at temperatures higher than 1000°C [8]. Nevertheless, after oxidation and cooling to room
5 temperature, important scale spallation generally occurs [7]. At 900°C, spallation only appeared on the niobium and
6 silicon rich areas. At 1000°C, scale spallation is present on the entire specimen surface indicating that this
7 temperature is too high to obtain an adherent chromia scale on the alloy surface. The comparisons between the 48
8 and 160h oxidation duration have shown that at 800 and 900°C a short oxidation duration (46h) is favourable to the
9 oxide scale adherence. It then appeared that the chromia scale never shows a perfect adherence on the alloy under
10 the tested conditions. In order to improve the chromia scale adherence previous works have proposed to introduce
11 lanthanum on the alloy surface as a La₂O₃ coating [9-13] or as an alloying element [14]. The present work deals with
12 the effect of lanthanum sol-gel coatings applied on the specimen surface before oxidation. Previous works have
13 already indicated that the argon annealing could improve the effect of the coating on the oxide scale adherence [15-
14 17]. These works were performed on alumina forming alloys. Lanthanum sol gel coating alone was not improving
15 the alumina scale adherence. The aim of the present work is to check if the argon annealing could improve the
16 effect of the coating on chromia forming alloy. Then, the sol-gel coating argon annealing as been tested at various
17 temperatures on a model 330 chromia forming alloy.
18

19 20 21 22 23 24 25 26 27 28 29 30 31 32 33 34 35 36 37 38 39 40 41 42 43 44 45 46 47 48 49 50 51 52 53 54 55 56 57 58 59 60 61 62 63 64 65

The model 330 alloy is an austenitic stainless steel elaborated at the Ecole des Mines de Saint Etienne, France. Table 1 gives the 330-alloy composition in weight %. 1 mm thick cylindrical specimens of around 13 mm diameter were abraded up to the 120-grit SiC paper, then degreased with ethanol and finally dried. This surface finishing was chosen in order to fit the surface state of the alloy used in industrial applications. The oxidation tests were performed at 900°C.

Kinetic results are obtained by thermogravimetric measurements under isothermal conditions. High temperature oxidation was performed during 46 hours in ambient air at the atmospheric pressure using a Setaram TGDTA 92-1600 microthermobalance. The oxide characterization was realized by *in situ* X-ray diffraction (XRD) tests. *In situ* XRD patterns were obtained by use of a high temperature MRI chamber installed in a Philips X'pert MPD diffractometer (copper radiation, $\lambda k_{\alpha} = 0.15406$ nm). The XRD conditions were 2 Θ scan, step 0.05° ranging from 10 to 80°, 2.5 s counting time. Each *in situ* XRD pattern is obtained within one hour in the 10-80° 2 Θ range. *In situ* XRD permit to follow the evolution of the oxide nature with time at the testing temperature. The oxide scale surface and cross-section morphologies have been observed in a JEOL 6400 scanning electron microscope (SEM) coupled with a LINK energy dispersive X-ray spectroscopy (EDXS). The EDXS point analyses were performed with an electron probe focused to a 1 μ m spot. The lanthanum sol-gel coating was performed using a 0.4 mol.l⁻¹ lanthanum hydroxide solution obtained from the precipitation of lanthanum hydroxide in 0.27 mol 28% ammonia. After filtration, the dissolution of the precipitate is obtained in the 69% nitric acid at 60°C [18]. The lanthanum sol-gel coatings are carried out by dipping the specimens during 2 s in the solution. Immediately after dipping, the specimens are dried in warm flowing air at 40°C during 1 min. The coating thickness is close to 0.5 μ m. After sol-gel coating, the argon annealing was performed in a horizontal quartz reaction tube. A heating ramp is applied at a rate of 5°C/min. until the 600, 800 or 1000°C annealing temperature is reached. The temperature is maintained during 2 h. Then, the specimen is cooled down at 5°C/min to room temperature. Before oxidation the XRD pattern indicates that the alloy is detected alone on the surface on non-annealed specimens. It means that the sol-gel coating is not sufficiently crystallised before the heating up of the specimen to be detected by XRD. Thermal cycling was performed in static laboratory air at atmospheric pressure in a horizontal tubular furnace. Two samples were placed at the same time into an alumina crucible to estimate the reproducibility. The thermal cycle consists in a 30 minutes exposure at high temperature, followed by 30 minutes at room temperature after air quenching. This frequency corresponds to industrial conditions in conveyor units. The weight change of the samples was determined after each cycle on a balance with an accuracy of ± 0.01 mg.

RESULTS

1
2
3
4 Kinetic results indicate that all lanthanum sol-gel coatings show a lower oxidation rate compared with blank
5 specimens in Figure 1. The lowest oxidation rate is observed with non-annealed specimen, oxidized at 900 °C. The
6 other sol-gel coated specimens show similar kinetic behaviours. Figure 2 shows the mass change curves versus the
7 number of 30 minutes cycles at 900°C for blank specimens and lanthanum sol-gel coated specimens. The
8 comparison of the kinetic curves show that lanthanum sol-gel coatings largely improve the oxide scale adherence.
9 On blank specimens spallation started after 50 cycles. On lanthanum sol-gel coated specimens the oxide scale is still
10 adherent after 250 cycles.
11

12
13
14
15
16
17 *In situ* X-ray diffraction patterns obtained on the blank 330 specimen oxidized, in air at 900°C indicate that the
18 oxide scale is only composed of $Mn_{1.5}Cr_{1.5}O_4$ (JCPDS 33-0892) and Cr_2O_3 (JCPDS 38-1479). Chromia is formed at
19 the beginning of the oxidation process. No phase transition is detected during the 46h oxidation and during cooling
20 to room temperature. The relatively high $Mn_{1.5}Cr_{1.5}O_4$ peaks intensities indicate that it is present at the external
21 interface even though it corresponds to a low amount of oxide grains observed on the SEM micrographs. The alloy
22 peaks are still detected after 46h oxidation because the scale is thin enough to permit its detection. Figure 3 shows
23 the *in situ* XRD patterns obtained during the 46 first hours oxidation at 900°C, in air, of the non-annealed sol-gel
24 coated alloy 330. Before oxidation, XRD shows that the alloy is detected alone on the surface. It indicates that the
25 sol-gel coating is not crystallised before the heating up of the specimen. At 900°C, XRD analyses show the initial
26 formation of $Mn_{1.5}Cr_{1.5}O_4$. The oxide Cr_2O_3 appears rapidly at the beginning of the oxidation. A lanthanum
27 containing oxide $LaCrO_3$ (JCPDS 33-0701) is also observed from the beginning of the oxidation process. This phase
28 is stable all along the test and is not transformed into another oxide. No phase transition is detected after cooling to
29 room temperature.
30

31
32 *In situ* XRD patterns, obtained during the 46 first hours oxidation at 900°C, in air, of the sol-gel coated 330, with
33 a 600°C argon annealing, show that $LaCrO_3$ is present on the surface. This oxide is present on the surface until the
34 end of the oxidation test. At 900 °C, XRD patterns show the growth of $Mn_{1.5}Cr_{1.5}O_4$ and Cr_2O_3 . Similar results are
35 obtained on 800 or 1000 °C argon annealed specimens. After argon annealing chromia and $LaCrO_3$ are present on
36 initial surface. Cr_2O_3 and the manganese chromite grow all along the oxidation test. $LaCrO_3$ is less detected with
37 time because it is incorporated inside the growing chromia scale. Figure 4 shows the specimen's surface scale
38 morphologies (SEI images x 3000). Blank specimens oxidized during 46h are covered by a chromia scale and
39 octahedral manganese chromite grains. Spalled areas are found on about 10% of the blank specimens surface. Where
40 the oxide scale spalled off, the underlying substrate surface is silicon rich (Figure 4a). With sol-gel coated
41 specimens, no scale spallation is observed on the surface (Figure 4b). The oxide scale is convoluted and the grain
42 size is small. The oxide grains are composed of chromia and lanthanum chromite. The surface micrograph obtained
43 after the 46 hours oxidation at 900°C in air of the sol-gel coated alloy 330, argon annealed at 600°C is presented on
44 Figure 4c. The biggest pyramidal grains correspond to manganese chromite. No spallation is observed on the
45 specimen's surface. The convoluted scale is mainly composed of chromia. SEM, surface micrographs obtained after
46 the 46 hours oxidation at 900°C in air of the sol-gel coated alloy 330, argon annealed at 800°C, are presented on
47 Figure 4d. No spallation is observed on the surface after oxidation at 900°C. The chromia scale is convoluted.
48 Surface micrographs obtained after the 46 hours oxidation at 900°C, in air, of the sol-gel coated 330, argon annealed
49 at 1000°C are presented on Figure 4e. In this case, little spalled areas are found on the surface. Lanthanum is still
50 found on the specimen's surface. It is also observed that the scale is convoluted. It is then concluded that the 1000°C
51 temperature argon annealing permits the incorporation of lanthanum inside the oxide scale.
52

53
54 The scale cross-section morphologies are presented on Figure 5. Blank specimens, oxidized during 46h, are
55 covered by a 3µm thick chromia scale (Figure 5a). On the sol-gel coated 330 specimen no scale spallation is
56 observed on the cross-section (Figure 5b). The oxide scale is 2µm thick and convoluted. $LaCrO_3$ is located at the
57 external interface (white areas on the BSE micrograph). The cross-section micrograph obtained after the 46 hours
58 oxidation at 900°C in air of the sol-gel coated 330, argon annealed at 600°C is presented on Figure 5c. No spallation
59 is observed on the specimen's cross-section. The very convoluted scale is mainly composed of a 2µm thick chromia
60 scale. Figure 5c shows the presence of lanthanum (white areas) inside the chromia scale. The cross-section
61
62
63
64
65

1
2
3
4 micrograph obtained after the 46 hours oxidation at 900°C in air of the sol-gel coated alloy 330, argon annealed at
5 800°C is presented on Figure 5d. Lanthanum is found inside the thin chromia scale. The 800°C temperature argon
6 annealing permits the incorporation of lanthanum inside the oxide scale. Cross-section micrographs obtained after
7 the 46 hours oxidation at 900°C in air of the sol-gel coated 330, argon annealed at 1000°C is shown on Figure 5e.
8 On this specimen, lanthanum is present close to the oxide/gas interface of the chromia scale.
9

10 11 12 13 DISCUSSION 14 15

16 Kinetic results have shown that lanthanum sol-gel coatings always lead to a lower oxidation rate compared to
17 blank specimens. All heat treatments lead to the same kinetic effect because lanthanum has been incorporated into
18 the oxide scale in the same way leading to similar scale structures. Paúl already showed this effect on austenitic
19 steels. This author proposed that a lanthanum sol-gel coating lowers the parabolic rate constants during oxidation at
20 900°C [19, 20]. It was also demonstrated that cerium ion implantation followed by an annealing process reducing
21 the defaults present in the alloy structure, leads to a lower oxidation rate at 900°C [19]. On the 330 alloy the oxide
22 scale protective character is confirmed by *in situ* XRD analysis (Figure 3), which shows the chromia scale
23 formation.
24

25 It also exhibits the manganese chromite growth from the beginning of the oxidation process at 900°C. SEM
26 surface analyses confirm the presence of Cr₂O₃ and Mn_{1.5}Cr_{1.5}O₄. On all sol-gel coated specimens, the chromia scale
27 growth occurs with the presence of LaCrO₃ from the starting point of the XRD *in situ* test. This oxide formation is
28 thermodynamically explained by a reaction between Cr₂O₃ and La₂O₃ according to the Cr₂O₃-La₂O₃ phase diagram
29 [22]. This oxide has also been obtained by mechanochemical synthesis by grinding constituent oxides by Zhang
30 [23]. The LaCrO₃ formation at high temperature on chromia forming alloys has been described by other authors [13,
31 24-27]. The present results indicate that the reaction between Cr₂O₃ and La₂O₃ occurs at the beginning of the
32 oxidation process on all coated specimens. As observed by SEM, argon annealing also lead to the lanthanum
33 incorporation inside the chromia scale during oxidation. *In situ* XRD shows that no structural changes occur along
34 the test and during cooling to room temperature. It is also demonstrated that the lanthanum chromite LaCrO₃ relative
35 peaks intensity is the same before an after cooling, indicating that this oxide remains unchanged after cooling. On
36 figure 5, it is observed that LaCrO₃ is mainly located close to the oxide/gas interface and that inward oxygen
37 diffusion contributes to the chromia scale growth. This scale structure develops with time during the oxidation
38 process and is not the result of a deformation during cooling to room temperature. The convolution mechanism
39 formation corresponds to the relaxation process of the lateral growth stresses generated in the chromia scale during
40 the oxidation process. It results from the formation of new oxide inside the chromia scale. Moreover, Figure 2 shows
41 that on blank specimens spallation started after 50 cycles whereas on lanthanum sol-gel coated specimens the oxide
42 scale is still adherent after 250 cycles. As proposed by other authors a convoluted scale structure suggests that the
43 cationic diffusion in chromia scale is lowered by the presence of lanthanum [28]. With lanthanum, the oxide scale is
44 adherent and shows a very convoluted aspect. This scale structure develops with time during the oxidation process
45 and is not the result of a deformation during cooling to room temperature [29-33]. The convolution mechanism
46 formation is not fully understood but it is proposed that during the oxidation process, lateral growth occurred in the
47 chromia scale [33]. It results from the formation of new oxide inside the chromia scale [33]. It can also be due to
48 growth stresses generated inside the chromia scale leading to a plastic deformation of the scale and the underlying
49 metallic substrate. Then, the growth stress relaxation in a thinner scale can explain the better scale adherence. Hou et
50 Al. proposed a mechanism explaining a scale convolution on a lanthanum implanted Fe-Cr-Al alloy [34]. They have
51 shown the distribution of local stress components. It appears that the convolution results from σ_{ox} which is the
52 compressive stress inside the oxide scale and σ_n which is the tensile stress normal to the alloy/oxide interface on
53 the convoluted oxide scale. According to Evans et al [35], σ_n increases with the curvature radius increase. Pint
54 indicated that during the scale growth, stresses develop inside the scale and at the oxide/alloy interface [28]. If the
55 scale adherence is maintained, growth stresses can be high enough to plastically deform the metallic substrate and
56 also influence the scale morphology. Interfacial voids can also play an important role on the stress development and
57 scale morphology. With, compressive stresses in the scale, an interfacial void can lead to a stress contribution
58
59
60
61
62
63
64
65

perpendicular to the alloy/oxide interface. On a hard metallic substrate, cavities can develop without scale buckling during its thickening. On the contrary, a smooth alloy can accommodate the stress increase by plastic deformation and buckling of the oxide scale. Some authors have shown that an yttrium sol-gel coating promotes a continuous silica scale formation at the internal interface on the alloy AISI 304 [36]. The silicon presence hinders the iron oxidation and the formation of non-protective iron oxides [37]. Even though alloy 330 contains 2.15 wt.% silicon no continuous silica scale formation was observed within the 46h oxidation at 900°C, in air because the oxidation duration is perhaps too short. The bad scale adherence on uncoated specimens can be also explained by the presence of a too high silicon amount in the alloy [34]. The absence of iron oxides in the scale can also be due to the fact that the alloy 330 is a 33.8% nickel-rich alloy.

CONCLUSION

Kinetic results have shown that lanthanum sol-gel coatings always lead to a lower oxidation rate compared to blank specimens. *In situ* XRD has shown that the lanthanum coating leads to the formation of LaCrO₃ by a reaction between La₂O₃ and Cr₂O₃. The scale structure suggests that the cationic diffusion in a chromia scale is lowered by the presence of lanthanum. On blank 330 specimens scale spallation is observed after cooling to room temperature. It appears that the 2-wt% silicon present in the alloy has no beneficial effect on the chromia scale adherence and that no continuous silica layer is formed. On the non-annealed sol-gel coated specimen and on the argon annealed specimens at 600, 800 and 1000°C, the oxide scale formed at 900°C, in air, is adherent after 48 hours isothermal oxidation. SEM micrographs revealed that the adherent oxide scales are convoluted and that lanthanum is close to the external interface. It results from the formation of new oxide inside the chromia scale due to an anionic and a cationic mixed diffusion process. Convolution can also be the result of growth stresses relaxation by plastic deformation of the scale. It appears that, argon annealing does not provide a significant improvement compared to non-annealed lanthanum coated specimens. Thermal cycling tests, performed on blank 330 and lanthanum sol-gel coated specimens without argon annealing, show that the scale adherence is largely improved by this coating. The results show that argon annealing of the lanthanum sol gel coating is not necessary to improve the scale adherence.

REFERENCES

1. C.M. Chun, T.A. Ramanarayanan, *Oxidation of Metals* **67**, 215 (2007).
2. F. Di Gabriele, F.H. Stott, Z. Liu, *Materials Science Forum* **461-464**, 545 (2004).
3. J. Zhang, D. J. Young, *Corrosion Science* **49**, 1450 (2007).
4. K.T. Voisey, Z. Liu, F.H. Stott, *Applied Surface Science* **252**, 3658 (2006).
5. Y. Nishiyama, K. Kitamura, N. Otsuka, *Materials Science Forum* **595-598**, 649 (2008).
6. R. Stevens, *Oxidation of Metals* **13**, 353 (1979).
7. H. Buscail, C. Issartel, C.T. Nguyen, A. Fleurentin, *Traitement Thermique* **394**, 31 (2009).
8. G.R. Holcomb, D.E. Alman, *Scripta Materialia* **54**, 1821(2006).
9. S. Fontana, R. Amendola, S. Chevalier, P. Piccardo, G. Caboche, M. Viviani, R. Molins, M. Sennour, *Journal of Power Sources* **171**, 652 (2007).
10. S.M.C. Fernandes, O.V. Correa, L.V. Ramanathan, *Journal of Thermal Analysis and Calorimetry* **106**, 541 (2011).
11. L.V. Ramanathan, M.F. Pillis, S.M.C. Fernandes, *Journal of Materials Science* **43**, 530 (2008).
12. Jong Seol Yoon, Jun Lee, Hae Jin Hwang, Chin Myung Whang, Ji-Woong Moon, Do-Hyeong Kim, *Journal of Power Sources* **181**, 281 (2008).
13. Gao-Min Zhao, Kun-Lin Wang, *Surface and Coating Technology* **190**, 249 (2005).
14. B. Gleeson, M. A. Harper, *Oxidation of Metals* **49**, 373 (1998).
15. H. Buscail, C.T. Nguyen, R. Cuff, C. Issartel, F. Riffard, S. Perrier, *Journal of Materials Science* **44**, 3968 (2009).
16. N. Karimi, H. Buscail, F. Riffard, F. Rabaste, R. Cuff, C. Issartel, E. Caudron, S. Perrier, *Materials Science Forum* **595-598**, 733 (2008).
17. C.T. Nguyen, H. Buscail, R. Cuff, C. Issartel, F. Riffard, S. Perrier, *Annales de Chimie Sciences des Matériaux* **33**, 33 (2008).
18. F. Czerwinski, J.A. Szpunar, *Journal of Sol-gel Science and Technology* **9**, 103 (1997).
19. A. Paúl and J. A. Odriozola, *Materials Science and Engineering A* **300**, 22 (2001).
20. A. Paúl, S. Elmrabet, J.A. Odriozola, *Journal of Alloys and Compounds* **323-324**, 70 (2001).

- 1
2
3
4 21. A. Paúl, S. Elmrbabet, F.J. Ager, J.A. Odriozola, M.A. Respaldiza, M.F. da Silva, J.C. Soares, *Oxidation of*
5 *Metals* **57**, 33 (2002)
6 22. R. Berjoan, *Revue Internationale Hautes Températures et Refractaires* **13**, 119 (1976).
7 23. Qiwu Zhang, Jinfeng Lu, Fumio Saito, *Powder Technology* **122**, 145 (2002).
8 24. A. Paúl, R. Sanchez, O.M. Montes, J.A. Odriozola, *Oxidation of Metals* **67**, 87 (2007).
9 25. Zigui Lu, Jiahong Zhu, Ye Pan, Naijuan Wu, Alex Ignatiev, *Journal of Power Sources* **178**, 282 (2008).
10 26. Wei Qu, Jian Li, Douglas G. Ivey, *Journal of Power Sources* **138**, 162 (2004).
11 27. J.H. Zhu, Y. Zhang, A. Basu, Z.G. Lu, M. Paranthaman, D.F. Lee, E.A. Payzant, *Surface and Coating*
12 *Technology* **177-178**, 65 (2004).
13 28. B.A. Pint, *Oxid. Met.* Vol. 45 (1996), p.1
14 29. F.H. Stott, G.C. Wood, *Materials Science and Engineering* **87**, 267 (1987).
15 30. F.H. Stott, G.C. Wood, J. Stringer, *Oxidation of Metals* **44**, 113 (1995).
16 31. R.G. Miner, V. Nagarajan, *Oxidation of Metals* **16**, 313 (1981).
17 32. V.K. Tolpygo, D.R. Clarke, *Acta Materialia* **46**, 5153 (1998).
18 33. F.A. Golightly, G.C. Wood, F.H. Stott, *Oxidation of Metals* **14**, 217 (1980).
19 34. P.Y. Hou, J. Stringer, *Journal de Physique IV* **C9**, 231 (1993).
20 35. A.G. Evans, G.B. Crumley, R.E. Demaray, *Oxidation of Metals* **20**, 193 (1983).
21 36. F. Riffard, H. Buscail, E. Caudron, R. Cueff, C. Issartel, S. Perrier, *Journal of Materials Science* **37**, 3925
22 (2002).
23 37. F.J. Pérez, M.J. Cristobal, M.P. Hierro, F. Pedraza, *Surface and Coating Technology* **120-121**, 442 (1999).
24
25
26
27
28

Figure captions:

29
30
31
32
33

34 **FIGURE 1.** Mass gain curves obtained on the alloy 330, oxidised in air, at 900°C. Comparison of the kinetic curves
35 obtained on the specimens: Blank specimens, lanthanum sol-gel coated without annealing, and
36 lanthanum sol-gel coated with argon annealing at 600, 800 or 1000°C.
37

38
39 **FIGURE 2.** Mass change curves versus the number of cycles (0.5h cycles), at 900°C; on blank and lanthanum sol-
40 gel coated 330 alloy specimens without argon annealing specimens.
41

42
43 **FIGURE 3.** In situ XRD patterns obtained for the 46 first hours oxidation at 900°C in air of the
44 lanthanum sol-gel coated alloy 330.
45

46
47
48 **FIGURE 4.** SEM surface micrographs of the specimens oxidized at 900°C, for 46 h, in air (SEI x 3000), effect of
49 Lanthanum coatings. a) Blank alloy 330, b) Alloy 330 sol-gel coated without argon annealing, c) Alloy
50 330 sol-gel coated with 600°C argon annealing, d) Alloy 330 sol-gel coated with 800°C argon
51 annealing, e) Alloy 330 sol-gel coated with 1000°C argon annealing.
52

53
54 **FIGURE 5.** SEM cross-section micrographs of the specimens oxidized at 900°C, for 46 h, in air (BSE). a) Blank
55 alloy 330, b) Alloy 330 sol-gel coated without argon annealing, c) Alloy 330 sol-gel coated with 600°C
56 argon annealing, d) Alloy 330 sol-gel coated with 800°C argon annealing, e) Alloy 330 sol-gel coated
57 with 1000°C argon annealing.
58
59
60
61
62
63
64
65

Figure 1

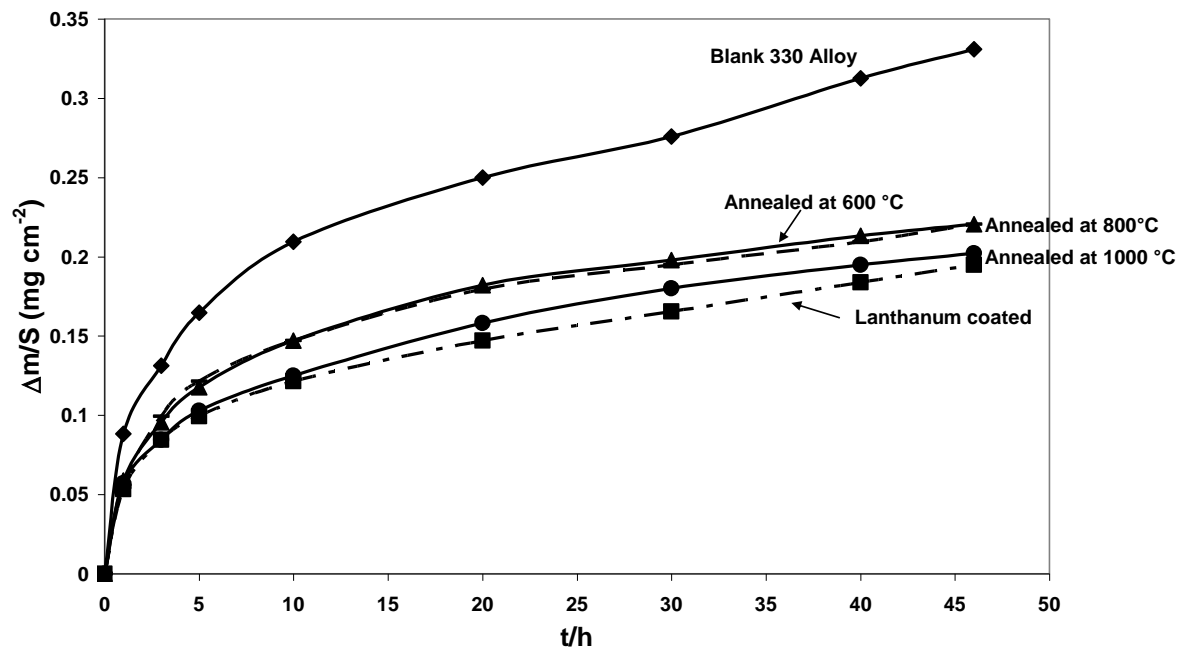


Figure 1: Mass gain curves obtained on the alloy 330 oxidised in air at 900°C. Comparison of the kinetic curves obtained on the specimens: Blank, sol gel coated without annealing, and sol gel coated with argon annealing at 600, 800 or 1000°C.

Figure 2

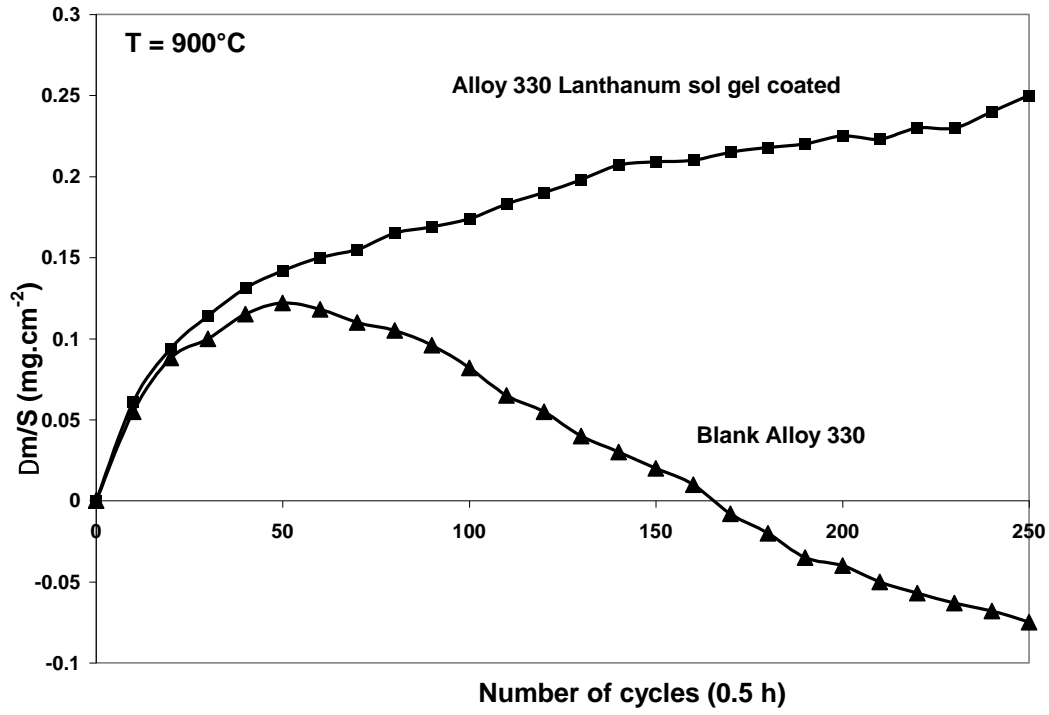


Figure 2: Mass change curves versus the number of cycles (0.5h cycles), at $900^{\circ}C$ on blank and lanthanum sol gel coated specimens without argon annealing specimens.

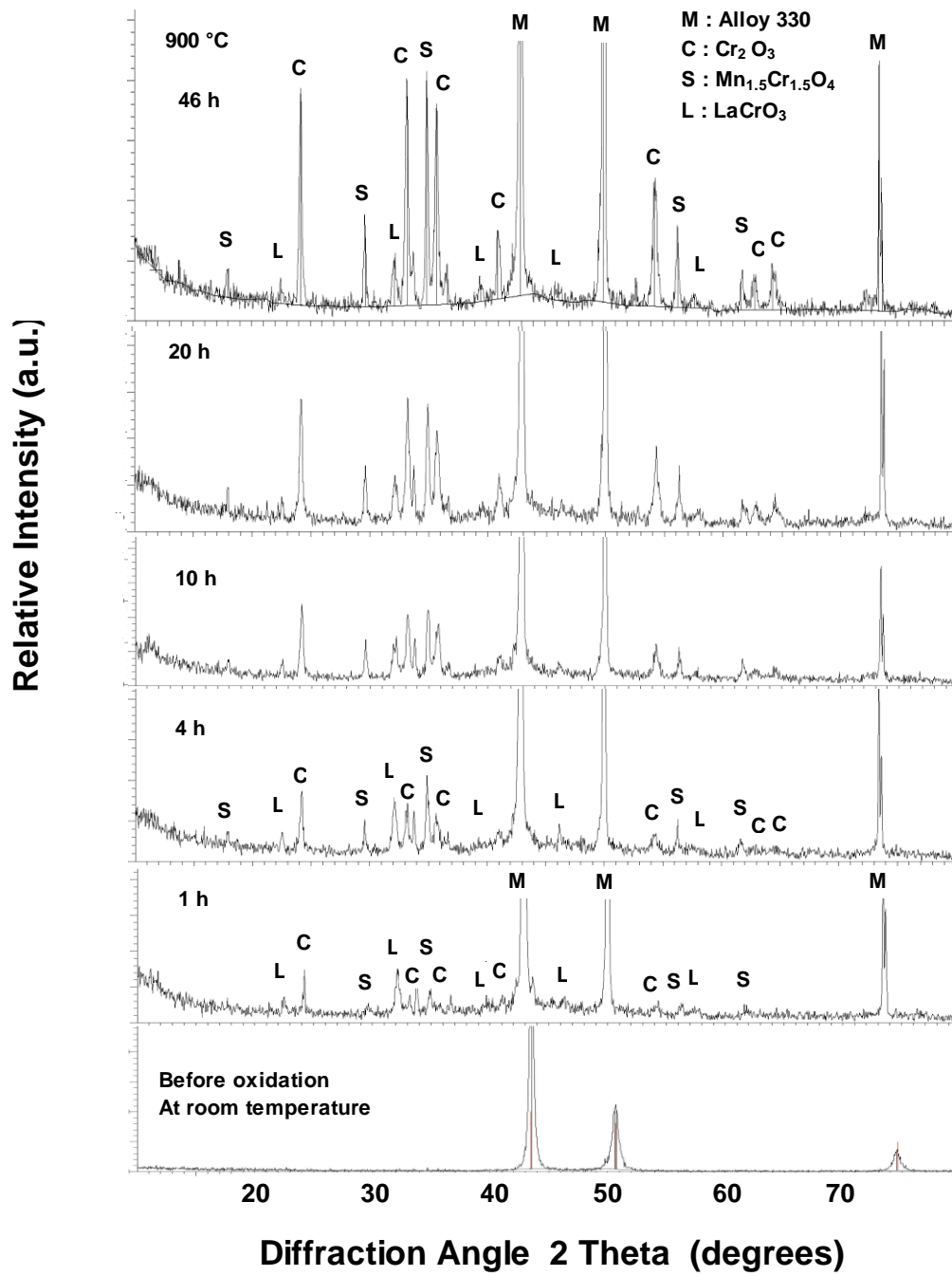


Figure 4: In situ XRD patterns obtained for the 46 first hours oxidation at 900 °C in air of the lanthanum sol gel coated alloy 330.

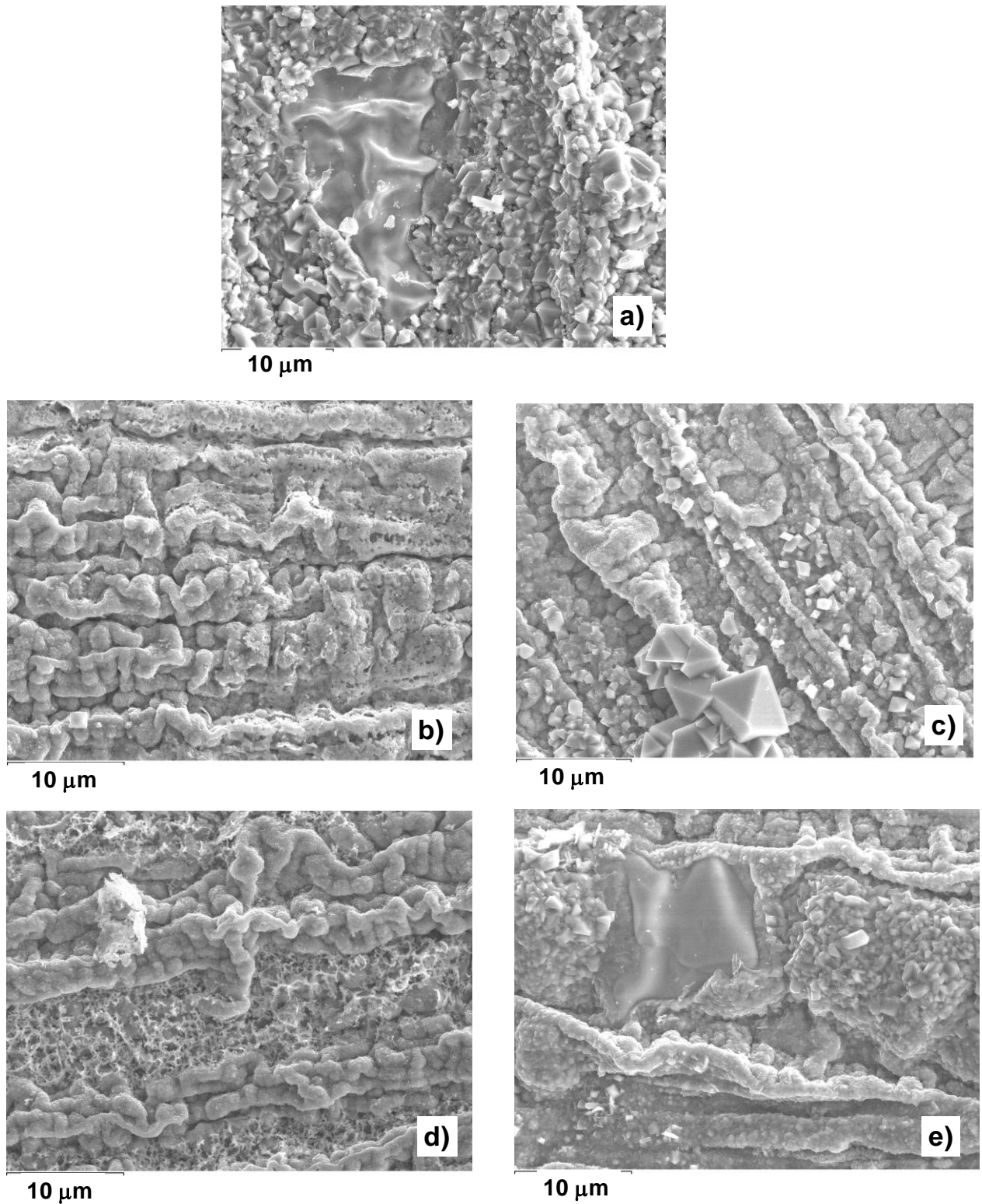


Figure 8: SEM surface micrographs of the specimens oxidized at 900°C, for 46 h, in air (SEI x 3000), effect of Lanthanum coatings. a) Blank alloy 330, b) Alloy 330 sol gel coated without argon annealing, c) Alloy 330 sol gel coated with 600 °C argon annealing, d) Alloy 330 sol gel coated with 800 °C argon annealing, e) Alloy 330 sol gel coated with 1000 °C argon annealing.

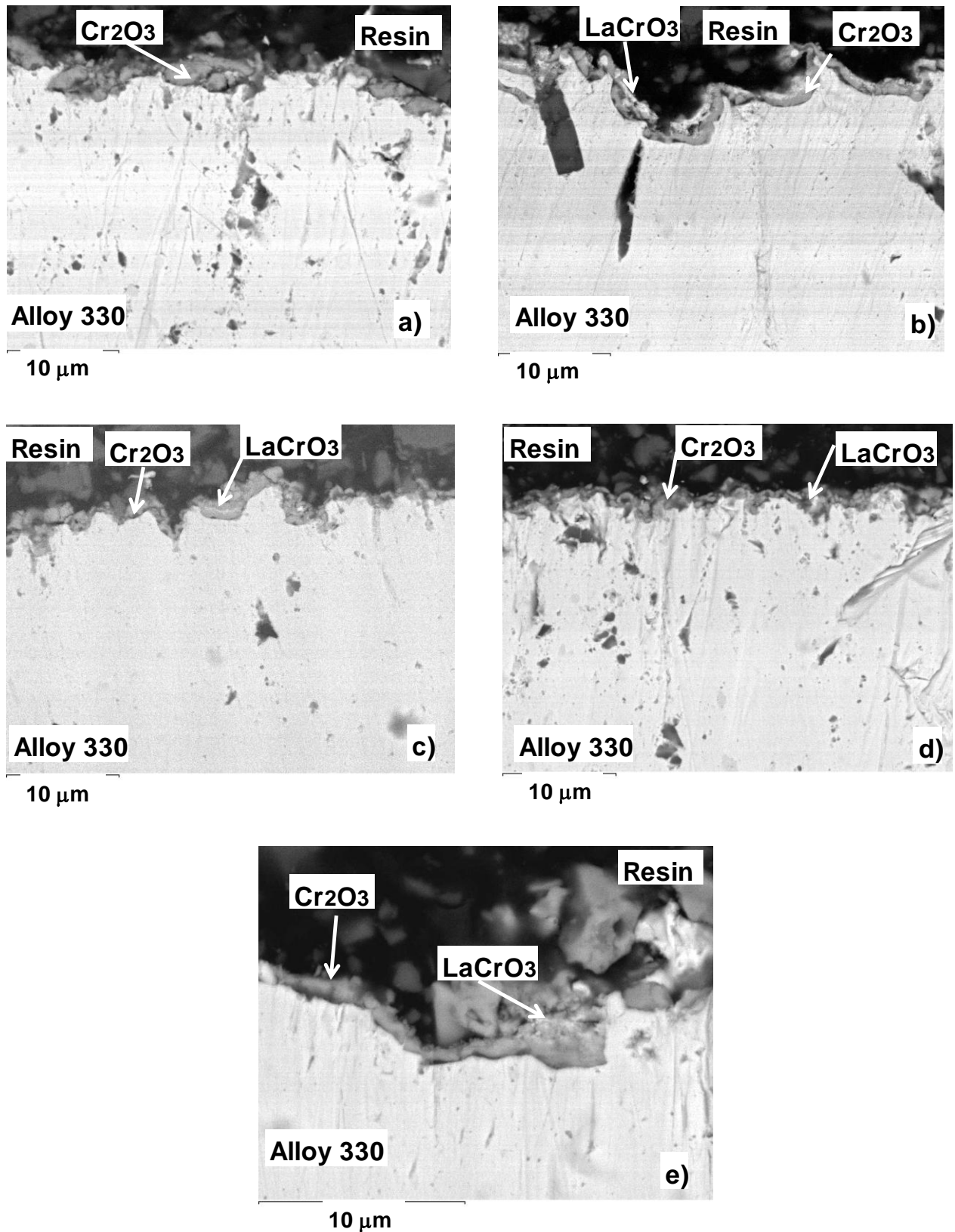


Figure 9: SEM cross-section micrographs of the specimens oxidized at 900°C, for 46 h, in air (BSE). a) Blank alloy 330, b) Alloy 330 sol gel coated without argon annealing, c) Alloy 330 sol gel coated with 600 °C argon annealing, d) Alloy 330 sol gel coated with 800 °C argon annealing, e) Alloy 330 sol gel coated with 1000 °C argon annealing.

Table 1

330 alloy composition (Fe-34Ni-21Cr-2Si) weight %.

Alloy 330	Fe	Ni	Cr	Si	Mn	Mo	Cu	C
wt. %	Bal.	33.80	21.10	2.15	0.70	0.20	0.20	0.05